3rd URSI AT-AP-RASC, Gran Canaria, 29 May – 3 June 2022

Time Reversal in Reverberating Environments for Electromagnetic Focusing in Biological Bodies

E. Colella(1), L. Bastianelli(1), V. Mariani Primiani(1) and F. Moglie(1)
(1) Università Politecnica delle Marche – DII – 60131 Ancona - Italy

Abstract

This paper proposes the time reversal as an electromagnetic focusing technique for improving deep biological tissues heating. The analysis occurred by full-wave FDTD simulations considering a body of a 6-year-old boy placed within a reverberant environment. The excitation was a pulse at the central frequency of 433.9 MHz. After the time reversal application, the distribution of the computed electromagnetic field shows excellent results in terms of strong spatial focusing within the human body. Examples are given for the head and limb.

1 Introduction

Biological tissue heating techniques are therapeutic medical tools that use ultrasound (US) and electromagnetic (EM) waves at high frequencies to heat biological tissues above the physiological temperature around 41-43°C. Hyperthermia, thermal ablation and diathermy are the main heating techniques used in the medical field for osteoarticular diseases and cancer treatments [1, 2]. US based techniques are mainly used for feating of the outermost biological tissues due to a low penetration range. This leaves more interest in EM heating techniques (EMHT) for deep tissue heating. EMHTs use microwaves whose frequency depends on the depth of the target tissue and on the International Telecommunication Union (ITU) Radio Regulations. Most commonly used frequencies are 434 MHz, 915 MHz and 2.45 GHz [3, 4, 5]. Despite the above mentioned techniques are effective, the focus of EM fields in an high non-homogeneity medium represents the greatest clinical challenge. Several years ago, the time reversal (TR) technique has been introduced for focusing acoustic and EM waves [7]. It consists of two main steps, in the first phase a transmitter (Tx) sends a EM signal which is recorded by a receiver (Rx), in the second phase, the recorded signal is flipped over time and re-emitted by the same Tx. At this point, the flipped and re-emitted signal focuses on the point where it was previously recorded, obtaining a similar signal to the one initially emitted [7, 8]. It has been shown that TR works even better in chaotic environments where the multiple scattering intensifies the focus of the EM wave [10, 11, 15]. Therefore, the reverberation chamber (RC) represents a great solution for TR applications. At this regard this paper proposes the TR in RC as an alternative tissue heating technique to improve EM wave focus within the human body.

2 Analysis description

In order to analyze the performance of the TR as tissue heating technique, numerical simulations have been performed based on the Finite-Difference Time-Domain (FDTD) method to reproduce computational electrodynamics [9]. The differential numerical modeling have been used to examine how the TR in RC affects the focusing of EM waves towards deep biological tissues.

2.1 Simulation set-up

The simulated domain was a RC sample by 1.0 mm cells as the tested biological tissues resolution. The walls of the RC have been made up by Perfect Electric Conductor (PEC) with zero resistance and zero tangent electric field to simulate a lossless environment with total reflection. The Tx antenna was a coaxial monopole consisting of 101 cells along the y-axis, placed in the lower left corner of the RC. The anatomical structures analyzed in the FDTD simulation were the head, the upper and the lower limbs of the Thelonius body map taken from the Foundation for Research on Information Technologies in Society [1] see figure 1. The biological volume to be heated by the TR was an internal cell of each body part. The biological tissue properties used in FDTD simulations were the relative electrical permittivity ε_r and the electrical conductivity σ [14]. The model selected for the dielectric data across the frequency range was a summation of 4-Cole-Cole expressions [12] as reported below:

$$\varepsilon_r = \varepsilon_\infty + \sum_{m=1}^{4} \frac{(\varepsilon_{s_m} - \varepsilon_\infty)}{1 + (j\omega\tau_m)^{1-\alpha_m}} - j\frac{\sigma}{\omega\varepsilon_0} \qquad (1)$$

where ε_s and ε_∞ are the static and infinite frequency dielectric constants, ε_0 is the permittivity of free space, ω is the angular frequency, τ is a time constant, σ is the conductivity and j the complex variable. In the following section, the the FDTD simulation procedure is reported.

[1] https://itis.swiss/virtual-population/tissue-properties/database/

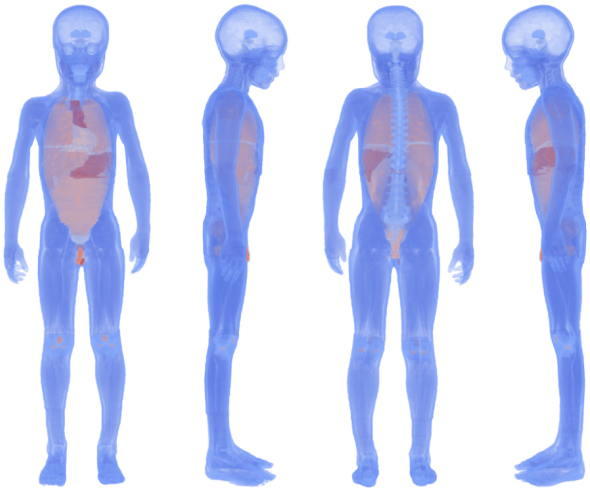

Figure 1. Thelonius is a 6 year old boy of 1.15 m height, weight 18.6 kg, BMI of 14.1 kg/m^2. DOI: 10.13099/VIP11004-03-0

2.2 FDTD simulation

The simulations took place inside the IRENE-KNL supercomputer of *Commissariat à l'énergie atomique et aux énergies alternatives* (CEA), France, featuring 828 Intel Knights Landing 7250 manycore nodes at 1.4 GHz with 68 cores per processor, for a total of 56,304 cores and a power of 2 Pflop/s, 96 GB of DDR4 memory and 16 GB of MCDRAM memory/node, integrating the Bull eXascale Interconnect Network (BXI). The FDTD code for any cell was implemented following the standard formulation [41] written in C-language code. The optimization of computer parallelism gains benefits when a simple staircase approximation was adopted for the PEC. Indeed, the tangential electric field was set to zero and the computational code did not deviate from the standard formulation. The timestep was set up at 6 ps with a total of 367553 iteratations for each simulation and 200 of total number of cycles. The maximum and minimum stability factors were 0.29 and 0.11, respectively, the maximum ratio λ/dx, λ/dy, λ/dz of 72.31 while their minimum ratio of 22.86. The Δz value for all the simulations was the cell size 3.6 mm while the stability factor for the fictitious one-dimensional transmission line is 0.33. The ratio λ/δ is 128, C_{11} (F/m) is equal to $1.0 \cdot 10^{-10}$ while L_{11} (H/m) is $2.6 \cdot 10^{-7}$. Z_0 (Ohm) is 51.6 while the phase velocity (m/s) is set to $2 \cdot 10^8$. Considering the system reported in fig., a generic signal $s(t)$ feeding the Tx, was a cosine signal modulated by a Gaussian pulse emitted in the RC, described as follows:

$$s(t) = \cos\left(2\pi f_0 (t - t_0)\right) \mathrm{e}^{-\frac{(t-t_0)^2}{t_g}} \tag{2}$$

where

$$t_g = \frac{12}{\left[\pi (f_{max} - f_{min})\right]^2} \tag{3}$$

and

$$t_0 = 3\sqrt{t_g} \tag{4}$$

with $f_{min} = 0.3839$ GHz, $f_{max} = 0.4839$ GHz and $f_0 = 0.4339$ GHz, with medium ratio 384.6. Given the impulse response $h(t)$ of the RC, the received signal at the cell the signal is to be focused:

$$u(t) = s(t) \otimes h(t) \tag{5}$$

where $\otimes$ denotes the time convolution. Applying the well known ordinary TR procedure [13], we apply the TR mirrored signal $u(-t)$ to the Tx achieving the reconstructed response:

$$s_r(t) = u(-t) \otimes h(t) \tag{6}$$

The reconstructed signal $s_r(t)$ was computed for any simulation in order to show how the re-emitted and flipped signal by the TR is mostly focused on the target cell. In the next session, the results of each simulation are reported.

3 Results

The simulation results were reported for the head and upper limb in terms of signal reconstruction and EM field distribution. As shown in the figure 2, the reconstructed signal in the head (top left) reproduces the emitted signal mainly in the center showing out of phase lobes at the ends. This affects the less focusing of the EM waves in the head as the EM field map for the head (top right) shows a less chaotic field distribution. According to the theory, the more chaotic the field, the better the signal reconstruction and the greater the heating at the target point. The results for the upper limb, instead, show a better signal reconstruction (lower left) without lobes at the ends and a more chaotic EM filed distribution in the upper limb (lower right). Furthermore, in the case of the upper limb, the reconstructed signal is perfectly in phase with the signal emitted, a symptom of a better reconstruction and a greater tissue heating.

4 Conclusions

In conclusion, the TR in RC reported excellent results in terms of heating of the biological tissues located deep within the human body thanks to a great focusing of the EM waves on the target volume. The absence of the diffusers have shown that the EM field distribution is less chaotic and therefore a lower heating. These results were predicted according to the TR theory [7, 11], giving credit to what has been simulated. In the future, it is possible to introduce diffusers into reverberating environments to increase the chaos of the EM field and therefore the focus of the EM waves.

5 Acknowledgements

We acknowledge PRACE for awarding us access to Joliot-Curie KNL at GENCI@CEA, France.

References

[1] R. B. Roemer, Engineering aspects of hyperthermia therapy. Annual Review of Biomedical Engineering, 1(1), 347-376.

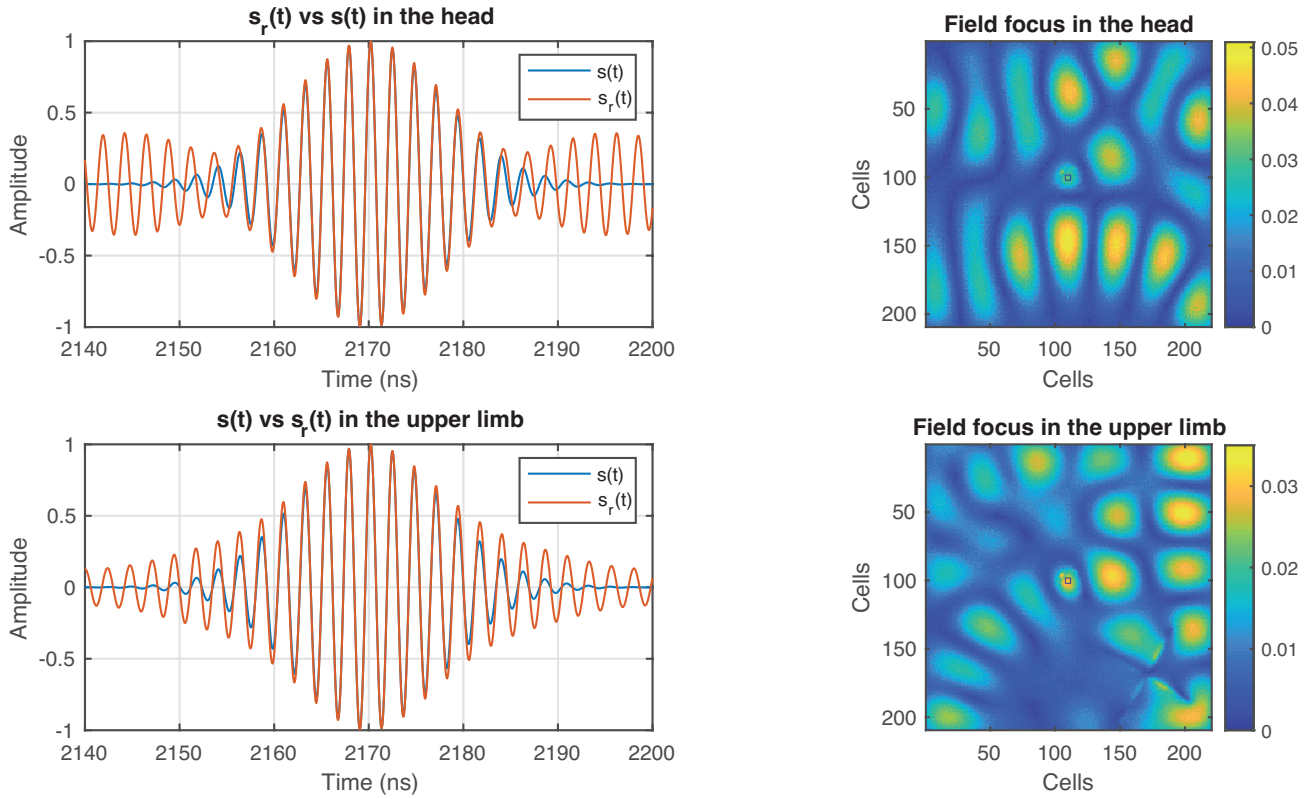

Figure 2. On the left $s_r(t)$ vs $s(t)$ are reported for the head and the upper limbs. On the right the EM field at the peak of the $s_r(t)$ are reported for the head, upper limbs.

[2] C.K. Chou, and R. Ren, Radio frequency hyperthermia in cancer therapy. The biomedical engineering handbook, 2.

[3] R. H. Johnson, A. W. Preece, and J. L. Green, Theoretical and experimental comparison of three types of electromagnetic hyperthermia applicator, Phys Med Biol, 35, 761, 1990.

[4] Y. Nikawa, and F. Okada, Dielectric loaded lens applicator for microwave hyperthermia, IEEE Trans Microwave Theory and Tech, 39, 1173, 1991.

[5] E. R. Lee, T. Wilsey, P. Tarczys-Hornoch, D. Kapp, P. Fessenden, A. W. Lohrbach, S. D. Prionas, Body conformable 915 MHz microstrip array applicators for large surface area hyperthermia, IEEE Trans Biomed Eng, 39, 470, 1992.

[6] C. Halperin Edward et al. Perez and Brady's Principles and Practice of Radiation Oncology. 2013.

[7] M. Fink (1992). Time reversal of ultrasonic fields. I. Basic principles. IEEE transactions on ultrasonics, ferroelectrics, and frequency control, 39(5), 555-566.

[8] G. Lerosey, J. De Rosny, A. Tourin, A. Derode, G. Montaldo, and M. Fink (2005). Time reversal of electromagnetic waves and telecommunication. Radio science, 40(6).

[9] A. Taflove (1988). Review of the formulation and applications of the finite-difference time-domain method for numerical modeling of electromagnetic wave interactions with arbitrary structures. Wave Motion, 10(6), 547-582.

[10] A. T. Frisco, L. Bastianelli, F. Moglie, and V. M. Primiani (2019, July). Time reversal in reverberation chambers: Application to lossy media. In 2019 IEEE International Symposium on Electromagnetic Compatibility, Signal and Power Integrity (EMC+ SIPI) (pp. 664-669). IEEE.

[11] B. Xiao, J. H. Yeh, T. Antonsen, E. Ott, and S.M. Anlage (2014, March). Time Reversal Experiments in Chaotic Cavities. In APS March Meeting Abstracts (Vol. 2014, pp. Z16-007).

[12] T. Said, and V. V. Varadan (2009, June). Variation of Cole-Cole model parameters with the complex permittivity of biological tissues. In 2009 IEEE MTT-S International Microwave Symposium Digest (pp. 1445-1448). IEEE.

[13] F. Rachidi, M. Rubinstein, and M. Paolone (Eds.). (2017). Electromagnetic time reversal: Application to EMC and power systems. John Wiley and Sons.

[14] C. Gabriel. Compilation of the Dielectric Properties of Body Tissues at RF and Microwave Frequencies, Re-

port N.AL/OE-TR- 1996-0037, Occupational and environmental health directorate, Radiofrequency Radiation Division, Brooks Air Force Base, Texas (USA), 1996.

[15] B. T. Taddese, G. Gradoni, F. Moglie, T. M. Antonsen, E. Ott, and S. M. Anlage (2013). Quantifying volume changing perturbations in a wave chaotic system. New Journal of Physics, 15(2), 023025.